Applied Soft Computing Journal 90 (2020) 106171

Contents lists available at ScienceDirect

Applied Soft Computing Journal

journal homepage: www.elsevier.com/locate/asoc

A novel fuzzy clustering algorithm by minimizing global and spatially constrained likelihood-based local entropies for noisy 3D brain MR image segmentation

Nabanita Mahata, Jamuna Kanta Sing *

Department of Computer Science & Engineering, Jadavpur University, Kolkata 700032, India

A R T I C L E I N F O

Article history:
Received 27 June 2019
Received in revised form 14 November 2019
Accepted 9 February 2020
Available online 15 February 2020

Keywords:
3D brain MR image segmentation
Clustering
Entropy
Image segmentation

A B S T R A C T

In this paper, we propose a novel fuzzy clustering algorithm by minimizing global and spatially constrained likelihood-based local entropies (FCMGsLE) for segmenting noisy 3D brain magnetic resonance (MR) image volumes. For each voxel, in order to measure uncertainties that arise while identifying its class, two different entropies are defined. In particular, they measure the amount of uncertainties in terms of global entropy using fuzzifier weighted global membership function and spatially constrained likelihood-based local entropy using fuzzifier weighted local membership function. To mitigate the effect of noise and intensity inhomogeneity (IIH) or radio frequency (RF) inhomogeneity, the local membership function is induced by spatially constrained likelihood measure. These entropies are minimized through a fuzzy objective function to obtain the cluster prototypes and membership functions. The final membership function is obtained by integrating these global and local membership functions using weighted parameters. The algorithm is assessed both qualitatively and quantitatively on ten 3D volumes of simulated and clinical brain MR image data having high levels of noise and intensity inhomogeneity and a synthetic 3D image volume with Rician noise. The simulation results reveal that the proposed algorithm outperforms several state-of-the-art algorithms devised in recent past when evaluated in terms of segmentation accuracy, Dice similarity coefficient, partition coefficient, and partition entropy

1. Introduction

The magnetic resonance imaging (MRI) technique is used in radiology to produce pictures of an anatomy for clinical diagnosis and treatment of diseases. However, due to noise, intensity inhomogeneity (IIH) or radio frequency (RF) inhomogeneity and partial volume effect, the intensity of a particular structural tissue varies across the image domain; resulting an image of low resolution and blurred tissue boundaries. As a result, the segmentation process becomes more difficult and challenging task. Although manual segmentation by trained experts is reliable, the process is time-consuming as well as susceptible to human errors and heavily depends on the expert's expertise. Thus, there is a strong need for computer aided segmentation method, which may yield accurate and robust results. The main factors that cause IIH include (i) static field strength, (ii) reduced radio frequency (RF) coil uniformity, (iii) RF penetration, (iv) gradient-driven eddy currents, and (v) patient movement at the time of image capturing [1–4].

Among the magnetic resonance (MR) images, brain MR images are extensively clinically studied due to its importance in patient treatment, such as detection of disease, therapy planning, post-therapy observation, etc. Reviews in brain MR image segmentation can be found in [3,5]. Segmentation of brain MR images into different tissue types usually helps to investigate the brain structure. It also helps the radiologists to detect any deformation in the brain, helping them for better treatment planning and diagnosis. Literature review suggests that brain MR images are usually segmented into three main structural tissues like, cerebrospinal fluid (CSF), gray matter (GM) and white matter (WM) [6–12]. It also suggests that among all the segmentation methods, the fuzzy c-means (FCM) clustering algorithm [6] and its variants are the most studied methods [7–12]. Ahmed et al. [7] presented a modified FCM algorithm for simultaneous segmentation of brain MR image and estimation of the IIH. It modified the objective function of the FCM algorithm to compensate the IIH while allowing the labeling of a pixel using the labels of pixels in its immediate neighborhood. It uses a parameter α, which is empirically selected to control the tradeoff between the original image and its median-filtered image. In addition, the algorithm computes the neighborhood iteration-by-iteration and thereby

* Corresponding author.
E-mail addresses: mahatanabanita1990@gmail.com (N. Mahata), jksing@ieee.org (J.K. Sing).

https://doi.org/10.1016/j.asoc.2020.106171
1568-4946/

takes more time to produce segmentation results. To mitigate the above difficulties, Cai et al. [8] proposed a fast and robust fuzzy c-means (FGFCM) algorithm using local information for image segmentation. It introduced a novel factor S_{ij} as the local similarity measure between the ith pixel and the neighboring jth pixel by incorporating local spatial and gray-level information. Wang et al. [9] proposed another improvement of the conventional FCM algorithm by an adaptive spatial information-theoretic fuzzy clustering (ASIFC) algorithm. It addressed two shortcomings of the FCM algorithm, namely (i) lack of spatial information and (ii) sensitivity to noise. The former one is addressed by incorporating a new similarity measure, which is computed from the immediate neighborhood with respect to a center pixel under consideration. Whereas, for the later one, it defines a mutual information (MI) maximization process to identify the reliable and unreliable (outlier) data points among the all data points or pixels and are processed separately. Chuang et al. [10] proposed sFCM algorithm, which also addressed the spatial information problem of the FCM algorithm, by incorporating local spatial information into the membership function. This spatial information is defined as the summation of the membership function in the immediate neighborhood of each pixel under consideration. The algorithm is capable of reducing the spurious blobs and less sensitive to noise. Another fuzzy algorithm using two fuzzifiers in the form of interval type-2 fuzzy set and a spatial constraint is proposed by Qiu et al. [11] for MR image segmentation. The algorithm resolves the issue of the FCM algorithm, where it fails to properly represent the pattern memberships using single fuzzifier, especially in the presence of noise and IIH in MR images. Pal et al. [12] proposed a possibilistic fuzzy c-means algorithm, where membership, possibilities and the cluster centers are generated simultaneously. In recent times, some modified FCM algorithms are devised for brain MR image segmentation [13–16]. In Mahata et al. [13], authors presented a fuzzy algorithm to estimate IIH and to segment brain MR image simultaneously. In the process, the algorithm uses a Gaussian function, characterizing the IIH and local contextual information, to undermine the effect of noise and IIH, in the objective function. In addition, for each pixel, it uses two membership functions; global and local into the objective function and they contribute to identify centers of the proper cluster prototypes. Authors in Kahali et al. [14] proposed a novel two-stage fuzzy multi-objective framework (2sFMoF) for segmenting 3D brain MR image volumes. It works in two stages. First, along with the global membership function it incorporates 3D spatial neighborhood information with the local membership function. Second, the cluster centers thus generated are considered as the initial cluster centers of a new 3D modified FCM algorithm, where the local voxel information is further incorporated to generate the final membership function and cluster prototypes. A modified FCM algorithm using scale controlled spatial information is proposed by Sing et al. [15] to segment noisy brain MR images. Here, a probability function is defined utilizing scale controlled spatial information from immediate square neighborhood of a pixel under consideration. It uses this parameter with the local membership function in the objective function. Later, by using a weighted function, it combines the local and global membership functions to generate the final membership function and uses to yield final cluster centers. Adhikari et al. [16] proposed a conditional spatial FCM (csFCM) algorithm for brain MR image segmentation. Apart from using global membership function, it introduces local membership function by incorporating auxiliary or conditional variables. These conditional variables are generated from neighboring spatial information and contribute in constructing cluster prototypes. By integrating the global and local membership functions using a weighted membership function it increases robustness to noise.

Apart from fuzzy logic based statistical methods, recently, some methods based on convolutional neural networks (CNNs) are proposed [17,18]. Pereira et al. [17] proposed a method for brain tumor segmentation in MR images using deep convolutional neural networks, exploiting small convolutional kernels. The architecture stacks more convolutional layers having same receptive fields as of bigger kernels. Moeskops et al. [18] proposed an automatic brain MR image segmentation method based on multi-scale CNN. It combines multiple patch and kernel sizes to learn multi-scale features, which estimate both the intensity and spatial characteristics. However, the main disadvantage of convolutional neural network is that it requires high computational time during its training phase.

The methods discussed so far do not use entropy while segmenting brain MR images. However, some authors proposed methods that use entropy in the objective function for classification of noisy data [19–23]. Yao et al. [19] proposed a fuzzy clustering method based on entropy to find all natural clusters from the input data. The algorithm selects the initial cluster centers based on minimum entropy associated with the data points. The algorithm does not need to revise entropy value for each data point after a cluster center is determined, thus saving some computational time. In Zarinbal et al. [20], relative entropy is incorporated into the objective function of fuzzy clustering algorithm to maximize the dissimilarity among all clusters. The relative entropy, using the membership values, works as a regularization function. This method is useful in case of heavy noisy data. Askari et al. [21] proposed a generalized entropy-based possibilistic fuzzy c-means algorithm for noisy data. It integrates fuzzy, possibilistic and entropy terms in the objective function. Kannan et al. [22] proposed a quadratic entropy based FCM algorithm by combining regularization function, quadratic terms, mean distance functions, and kernel distance functions. The algorithm is evaluated on time series data. Gharieb et al. [23] proposed a modified FCM algorithm by combining both local data and membership function into the objective function. It uses two membership relative entropy (MRE) functions to incorporate local membership function. Whereas, the local data information is incorporated using a weighted distance computed from the local neighborhood.

In this paper, we propose a fuzzy clustering algorithm by minimizing global and spatially constrained likelihood-based local entropies for segmenting noisy 3D brain MR image volumes. Since the brain MR images have low resolution and blurred tissue boundaries, we assume that in a small neighborhood around the unsharp tissue boundaries, the voxels possesses strong correlation to become member of a specific tissue type and highest amount of class uncertainty. In other words, these voxels characterize similar properties with respect to a tissue region. We define two entropies for each voxel using its global and local membership functions weighted by the fuzzifier parameter. In particular, these entropies measure the amount of uncertainty by considering the intensity distribution globally in the 3D image domain and also in the spatially constrained local neighborhood. The cluster prototypes and membership functions are obtained by minimizing these entropies through a fuzzy objective function. The final membership function is obtained by integrating these global and local membership functions using weighted parameters. We have tested the method on six simulated T1-weighted brain MR image volumes having high levels of noise and IIH, four clinical brain MR image volumes and a synthetic image volume with Rician noise. From the qualitative and quantitative investigations, we find that the proposed algorithm is better than several the state-of-the-art algorithms.

The rest of the paper is organized as follows. Section 2 presents the proposed fuzzy clustering algorithm. In Section 3, we have investigated the performance of the proposed algorithm and compared with several state-of-the-art algorithms. Finally, Section 4 draws the conclusions.

2. Novel fuzzy clustering algorithm by minimizing global and spatially constrained likelihood-based local entropies

This section describes the proposed fuzzy clustering algorithm by minimizing global and spatially constrained likelihood-based local entropies (FCMGsLE) for segmentation of noisy 3D brain MR image volumes. It differs from the entropy based fuzzy clustering algorithms discussed earlier in many aspects. First, the proposed algorithm aims to segment a 3D brain MR image volume as a whole in the presence of high noise and IIH. Second, it exploits two membership functions; global and local, which is constrained by a possibility factor using local neighborhood information. Third, it incorporates global entropy and local entropy using fuzzifier weighted global and local membership functions, respectively to measure the uncertainty while classifying a voxel. Fourth, it resolves the tradeoff between the global and local factors using a regularizing parameter.

Due to noise and IIH, the voxel intensity distribution of a specific tissue is irregular across the 3D brain MR image volume, resulting irregular visual texture. For this inherited artifacts, uncertainty arises in the process of predicting the class of each voxel. The maximum uncertainty arises at the unsharp tissue boundaries. To mitigate this problem, we have introduced entropy to define this uncertainty associated with each voxel. In particular, for better representation of uncertainty, two entropies are defined; (i) global entropy using fuzzifier weighted global membership function and (ii) spatially constrained likelihood-based local entropy using fuzzifier weighted local membership function. The global entropy specifies the underline uncertainty in the whole 3D image space; whereas, the local entropy specifies it in the local neighborhood. In particular, this mechanism makes the entropies capable of handling more uncertainty. The global and local membership functions as well as the said global and local entropies are incorporated into the fuzzy objective function with a regularizing parameter to resolve the tradeoffs. The cluster prototypes, global and local membership functions are obtained by minimizing the objective function. The global and local membership functions are treated as two unrelated or independent parameters and they contribute proportionally to form the final cluster centers. Therefore, the final membership function is obtained by weighted combination of these two membership functions. The 3D brain MR image volume is segmented based on this final membership function. Fig. 1 shows the overall workflow of the proposed FCMGsLE algorithm. It takes a noisy 3D brain MR image volume as an input and segments into three image volumes, corresponding to CSF, GM and WM soft tissue regions.

The proposed fuzzy algorithm may be formulated using a 3D brain MR image volume of size $X \times Y \times Z$, where X, Y and Z represent the height (row), width (column), and depth (number of images), respectively. Let there are C different main tissue regions, which are to be segmented. Therefore, the objective function of the FCMGsLE algorithm is defined as follows:

$$\begin{aligned} J_{FCMGsLE} = & \sum_{i=1}^{C}\sum_{l=1}^{Z}\sum_{j=1}^{X}\sum_{k=1}^{Y}[\alpha \mu_{i_{jkl}}^{m}(d_{i_{jkl}})^2 + (1-\alpha)\, u_{i_{jkl}}^{m}(f_{i_{jkl}})^{-1}(\bar{d}_{i_{jkl}})^2] \\ & - \alpha \sum_{l=1}^{Z}\sum_{j=1}^{X}\sum_{k=1}^{Y}\sum_{i=1}^{C} \mu_{i_{jkl}}^{m} \ln(\mu_{i_{jkl}}^{m}) \\ & - (1-\alpha)\sum_{l=1}^{Z}\sum_{j=1}^{X}\sum_{k=1}^{Y}\sum_{i=1}^{C} u_{i_{jkl}}^{m} \ln(u_{i_{jkl}}^{m}) \end{aligned} \quad (1)$$

subject to the following two constraints:

$$\sum_{i=1}^{C}\mu_{i_{jkl}} = 1 \text{ and } \quad \sum_{i=1}^{C} u_{i_{jkl}} = 1 \qquad \forall j,k,l \quad (2)$$

where $\mu_{i_{jkl}}$ and $u_{i_{jkl}}$ denote the global and local membership values, respectively of the voxel a_{jkl} for ith cluster. The parameter m (usually > 1.0) is the fuzzifier and may be selected empirically. A comparative study for selecting m can be found in Wu [24]. α ($0.0 < \alpha \leq 1.0$) is the regularizing parameter. $d_{i_{jkl}}$ represents the Euclidean distance between the voxel a_{jkl} and center of the ith cluster t_i. $\bar{d}_{i_{jkl}}$ denotes the mean of the Euclidean distances between the neighboring voxels of a_{jkl} and center of the ith cluster t_i. $f_{i_{jkl}}$ is the likelihood or possibility measure of belongingness into the ith cluster for the voxel a_{jkl} by using constrained local neighborhood information.

The parameters $d_{i_{jkl}}$, $\bar{d}_{i_{jkl}}$ and $f_{i_{jkl}}$ are defined by the following equations:

$$(d_{i_{jkl}})^2 = \left\| a_{jkl} - t_i \right\|^2 \quad \forall i,j,k,l \quad (3)$$

$$(\bar{d}_{i_{jkl}})^2 = \frac{1}{N}\sum_{x_{jkl}\in N_{jkl}} \left\| x_{jkl} - t_i \right\|^2 \quad \forall i,j,k,l \quad (4)$$

$$f_{i_{jkl}} = \frac{\sum_{x_{jkl}\in N_{jkl}}(\mu_{i_{jkl}} x_{jkl})}{\sum_{x_{jkl}\in N_{jkl}} x_{jkl}} \quad \forall i,j,k,l \quad (5)$$

where N and N_{jkl} denote the total number of neighboring voxels and constrained neighborhood, respectively with respect to the center voxel a_{jkl}. x_{jkl} denotes the corresponding neighboring voxel.

The aim of the first term of (1) is to minimize the products of global membership functions weighted by the fuzzifier and the Euclidean distances in the 3D image space, where the distance is inversely proportional to the membership function. The second term introduces the local membership function influenced by the reciprocal of a possibility measure using spatially constrained local neighborhood information. The aim of this term is similar to that of the first term, except that it works on local spatial neighborhoods across the whole 3D image space. A regularizing parameter is introduced to resolve the tradeoff between these two terms. The third and fourth terms define the global and local entropies, respectively with respect to class uncertainty associated with each voxel.

The objective of the proposed algorithm is to minimize the above four terms by considering the associated constraints; resulting the iterative equations of the necessary parameters. After rewriting (1) by incorporating the two constraints using Lagrange multipliers, the final iterative equations of the parameters $\mu_{i_{jkl}}$, $u_{i_{jkl}}$ and t_i can be found by performing its partial derivations with respect to $\mu_{i_{jkl}}$, $u_{i_{jkl}}$ and t_i, respectively and equating them to zero. The final iterative equations are found to be as follows:

$$\mu_{i_{jkl}} = \frac{1}{\sum_{r=1}^{C}\left(\frac{\alpha[(d_{i_{jkl}})^2 - \ln\left(\mu_{i_{jkl}}^{m}\right) - 1]}{\alpha[(d_{r_{jkl}})^2 - \ln\left(\mu_{r_{jkl}}^{m}\right) - 1]}\right)^{\frac{1}{m-1}}} \quad \forall i,j,k,l \quad (6)$$

$$u_{i_{jkl}} = \frac{1}{\sum_{r=1}^{C}\left(\frac{(1-\alpha)[(f_{i_{jkl}})^{-1}(\bar{d}_{i_{jkl}})^2 - \ln\left(u_{i_{jkl}}^{m}\right) - 1]}{(1-\alpha)[(f_{i_{jkl}})^{-1}(\bar{d}_{r_{jkl}})^2 - \ln\left(u_{r_{jkl}}^{m}\right) - 1]}\right)^{\frac{1}{m-1}}} \quad \forall i,j,k,l \quad (7)$$

$$\begin{aligned} t_i &= \left.\frac{\sum_{l=1}^{Z}\sum_{j=1}^{X}\sum_{k=1}^{Y}\{\alpha \mu_{i_{jkl}}^{m} a_{jkl} + (1-\alpha)\, u_{i_{jkl}}^{m}(f_{i_{jkl}})^{-1}\bar{a}_{jkl}\}}{\sum_{l=1}^{Z}\sum_{j=1}^{X}\sum_{k=1}^{Y}\{\alpha \mu_{i_{jkl}}^{m} + (1-\alpha)\, u_{i_{jkl}}^{m}(f_{i_{jkl}})^{-1}\}}\right|_{\bar{a}_{jkl}} \\ &= \frac{1}{N}\sum_{x_{jkl}\in N_{jkl}} x_{jkl} \quad \forall i \end{aligned} \quad (8)$$

Once the global and local membership values are obtained, we derive the final membership value $g_{i_{jkl}}$ using the following

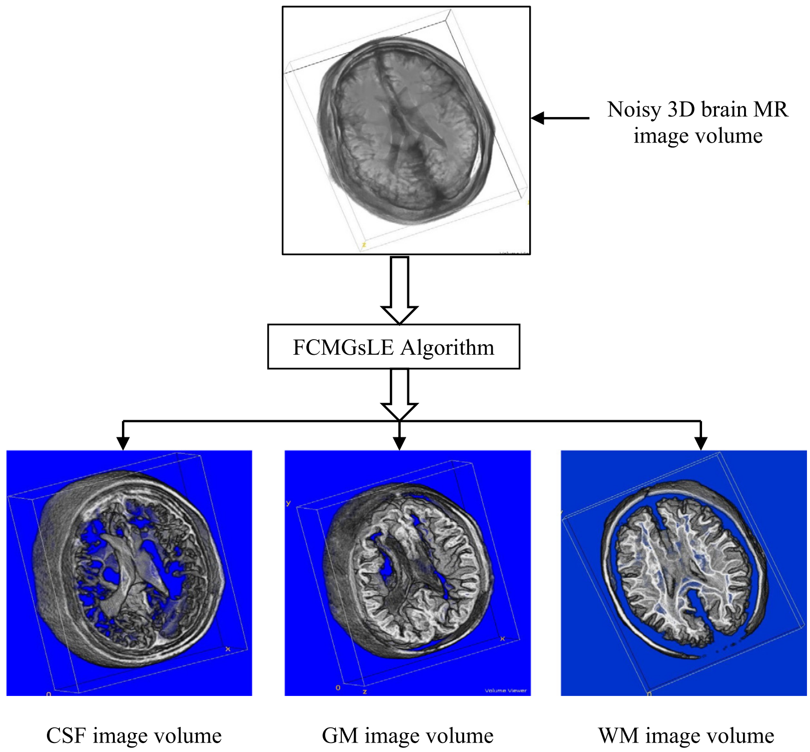

Fig. 1. Overall workflow of the FCMGsLE algorithm.

weighted equation.

$$g_{ijkl} = \frac{\left(\mu_{ijkl}\right)^p \left(u_{ijkl}\right)^q}{\sum_{r=1}^{C} \left(\mu_{rjkl}\right)^p \left(u_{rjkl}\right)^q} \quad \forall i, j, k, l \tag{9}$$

where p and q $(1 \le p, q \le 3)$ are the weighting parameters to control the effect of the global and local membership values, respectively.

The proposed FCMGsLE algorithm is summarized as follows:

The FCMGsLE Algorithm:
Input: One 3D brain MR image volume $\boldsymbol{A}$ having height X, width Y and depth Z with C distinct clusters or tissue regions or objects.
Output: Final cluster centers $\boldsymbol{T}$, membership matrix $\boldsymbol{G}$ and segmented 3D image volumes $\boldsymbol{B}_i$, $i = 1, 2, \ldots, C$.

Steps:

1. Set the parameters m, p, q and error ε.
2. Initialize the cluster centers $t_i^{(0)}$ $\forall i$, global membership values $\mu_{ijkl}^{(0)}$ $\forall i, j, k, l$ and local membership values $u_{ijkl}^{(0)}$ $\forall i, j, k, l$. The cluster centers can be initialized based on the information available from the image histogram and accordingly the global and local membership values can be initialized.
3. Set iteration $n = 0$.
4. *Repeat*

   i. Find the new global membership values using the following equation.

   $$\mu_{ijkl}^{(n+1)} = \frac{1}{\sum_{r=1}^{C} \left(\frac{\alpha[(d_{ijkl})^2 - \ln\left(\mu_{ijkl}^m\right) - 1]}{\alpha[(d_{rjkl})^2 - \ln\left(\mu_{rjkl}^m\right) - 1]} \right)^{\frac{1}{m-1}}} \quad \forall i, j, k, l$$

   ii. Find the new local membership values using following equation.

   $$u_{ijkl}^{(n+1)} = \frac{1}{\sum_{r=1}^{C} \left(\frac{(1-\alpha)[(f_{ijkl})^{-1}(\bar{d}_{ijkl})^2 - \ln\left(u_{ijkl}^m\right) - 1]}{(1-\alpha)[(f_{ijkl})^{-1}(\bar{d}_{rjkl})^2 - \ln\left(u_{rjkl}^m\right) - 1]} \right)^{\frac{1}{m-1}}} \quad \forall i, j, k, l$$

   iii. Find the new cluster centers as follows:

   $$t_i = \frac{\sum_{l=1}^{Z}\sum_{j=1}^{X}\sum_{k=1}^{Y}\{\alpha \mu_{ijkl}^m a_{jkl} + (1-\alpha)\, u_{ijkl}^m (f_{ijkl})^{-1} \bar{a}_{jkl}\}}{\sum_{l=1}^{Z}\sum_{j=1}^{X}\sum_{k=1}^{Y}\{\alpha \mu_{ijkl}^m + (1-\alpha)\, u_{ijkl}^m (f_{ijkl})^{-1}\}} \quad \forall i$$

5. *Until* $\left\| t_i^{(n+1)} - t_i^{(n)} \right\| < \varepsilon\ \forall i.$
6. Calculate the final membership values by the following weighted membership function.

   $$g_{ijkl} = \frac{\left(\mu_{ijkl}\right)^p \left(u_{ijkl}\right)^q}{\sum_{r=1}^{C} \left(\mu_{rjkl}\right)^p \left(u_{rjkl}\right)^q} \quad \forall i, j, k, l$$

7. Return the cluster centers $\boldsymbol{T} = \{t_1, t_2 \ldots, t_C\}$ and membership matrix $\boldsymbol{G} = \{g_{ijkl}\}$ $\forall i, j, k, l$.
8. Determine the clusters of the voxels $\{a_{jkl}\}$ $\forall j, k, l$ as follows and return the segmented 3D image volumes $\boldsymbol{B}_i$ $\forall i$:

   $$cluster\left(a_{jkl}\right) = \underset{i}{\arg max}\left\{g_{ijkl}\right\} \quad i = 1, 2, \ldots, C$$

3. Experimental results and discussion

The performance of the proposed FCMGsLE algorithm is extensive studied on six simulated and four clinical 3D brain MR image volumes, and a synthetic image volume with Rician noise. We have used T1-weighted brain MR image volumes, as this modality is most commonly use in the clinical studies and the ones typically effected by IIH. The brain image volumes are segmented into four regions ($C = 4$) including the three main constituents of the brain, corresponding to (i) cerebrospinal fluid (CSF), (ii) gray matter (GM), (iii) white matter (WM) and background (BG).

The FCMGsLE algorithm with $m = 2.5$, $C = 4$, $p = 1$ and $q = 3$ in segmenting these image volumes is studied. These parameters are selected empirically. The neighborhood window of size $3 \times 3 \times 3$ is also empirically selected and used to compute the mean Euclidean distance $\bar{d}_{i_{jkl}}$, mean voxel $\bar{a}_{jkl}$ and the measure of possibility factor $f_{i_{jkl}}$ for a voxel to belong into a cluster. The investigation is performed both qualitatively and quantitatively. In this regard, the investigation is performed by analyzing some performance indices, such as (i) segmentation accuracy (SA), (ii) Dice similarity coefficient (DSC) or Dice coefficient, (iii) partition coefficient (V_{pc}) and (iv) partition entropy (V_{pe}). For better understanding of the analysis, we have discussed these indices in the following sections.

The segmentation accuracy (SA) of a clustering algorithm can be defined as the ratio of the number of correctly classified voxels and the actual number of corresponding voxels in the ground truth. The algorithm is said to be better if the value of SA is closer to 1.0 and in ideal case its value is equals to 1.0. Let A_i represents the set of the voxels correctly classified by the algorithm into the ith cluster (here, distinct region or tissue) and B_i is the set of the voxels present in the ground truth of the ith cluster. Then, the SA for cluster i, denoted as SA(i), is defined by the following equation [9,14]:

$$SA(i) = \frac{|A_i \cap B_i|}{|B_i|} \tag{10}$$

Dice similarity coefficient (DSC) or Dice coefficient is a very important performance index as it measures the spatial overlap between the segmentation result and the ground truth. The DSC is also known as the similarity index ρ. Let C is the total number of clusters, the set of voxels of cluster i in the segmented image volume is A_i. Similarly, the set of voxels of cluster i in the ground truth image volume is represented by B_i. The Dice similarity coefficient or Dice coefficient is defined as follows [11,16]:

$$DSC = \frac{1}{C} \sum_{i=1}^{C} \frac{2\,|A_i \cap B_i|}{|A_i| + |B_i|} \tag{11}$$

For ideal segmentation, the value of DSC is 1.0. However, value closer to 1.0 is considered as better.

To evaluate performance of a fuzzy clustering algorithm, clustering validity functions are widely considered. Among them, the partition coefficient V_{pc} is an important index as it measures the confidence of the algorithm while classifying the patterns (here voxels). The value of V_{pc} lies in [0.0, 1.0]. However, for an ideal clustering, V_{pc} is 1.0 and its higher value considered as better. It is defined as follows [6,11,16]:

$$V_{pc} = \frac{\sum_{l=1}^{Z} \sum_{j=1}^{X} \sum_{k=1}^{Y} \sum_{i=1}^{C} \left(g_{i_{jkl}}\right)^2}{X \times Y \times Z} \tag{12}$$

Partition entropy V_{pe} is another important index under the clustering validity functions. It measures the uncertainty while classifying the voxels into correct clusters and negating into other clusters. In an ideal case, the V_{pc} is 0.0 and is defined by the following equation [6,11,16].

$$V_{pe} = \frac{-\sum_{l=1}^{Z} \sum_{j=1}^{X} \sum_{k=1}^{Y} \sum_{i=1}^{C} \left(g_{i_{jkl}} \ln g_{i_{jkl}}\right)}{X \times Y \times Z} \tag{13}$$

3.1. Parameter setting of the FCMGsLE algorithm

The performance of the FCMGsLE algorithm depends on the parameters m, p and q. This section presents a performance analysis by varying these parameters to determine the best combination. Fig. 2 shows the comparative DSC values of the algorithm by varying p and q with $m = 2.0$ on a simulated 3D brain MR image volume with 9% noise and 40% IIH (highest combination of noise and IIH) from the BrainWeb [25] database. The results show that $(p, q) = (1, 3)$ provides highest DSC value as 0.77316. Similarly, Fig. 3 shows the DSC values of the algorithm by varying m with $(p, q) = (1, 3)$, where $m = 2.5$ yields best DSC value as 0.77317. Therefore, the algorithm is tested with $m = 2.5$, $p = 1$ and $q = 3$ for the remaining experiments.

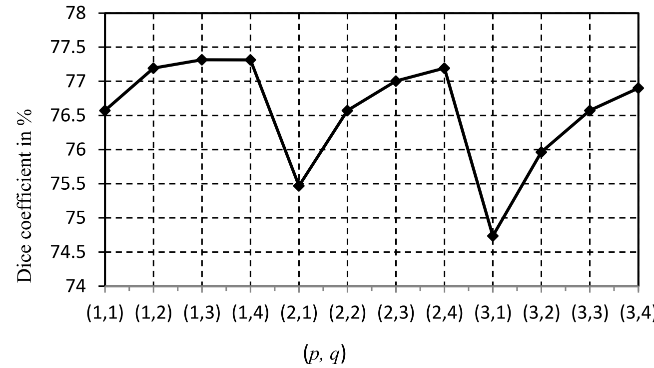

Fig. 2. Performance of the FCMGsLE algorithm by varying (p, q) with $m = 2.0$ in terms of Dice coefficient (DSC).

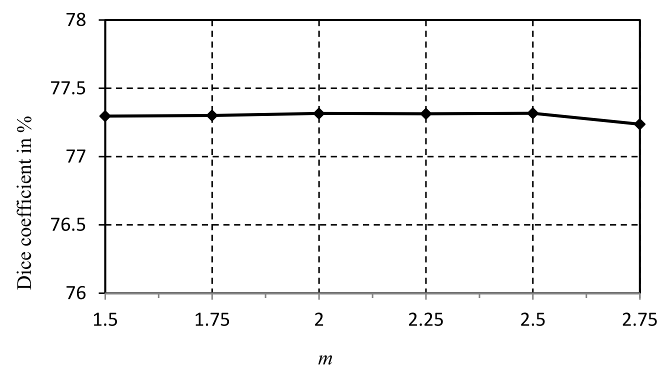

Fig. 3. Performance of the FCMGsLE algorithm by varying m with (p, q) = (1, 3) in terms of Dice coefficient (DSC).

3.2. Qualitative analysis

This study presents the performance of the proposed FCMGsLE algorithm by displaying the segmented image volumes.

3.2.1. Simulated 3D brain MR image volumes

We have downloaded the simulated brain MR image volumes from the BrainWeb [25] by varying high amount of noise (5%–9%) and IIH (20%–40%). Each image volume is of size (height × width × depth) 181 × 217 × 181 with voxel thickness of 1 mm × 1 mm × 1 mm. Among the six image volumes, a T1-weighted simulated 3D brain MR image volume, having 9% noise and 40% IIH (maximum amount of noise and IIH), consisting of 51 images or slices (slices 50–100 are considered as they have fair amount of CSF, GM and WM regions) from BrainWeb is shown in Fig. 4(a). The segmented image volumes of the CSF, GM and WM regions are shown in Fig. 4(e), (g) and (i), respectively. For further understanding about the shapes and structures of these regions, the bottom two-thirds of these volumes are presented in Fig. 4(f), (h) and (j), respectively. To understand the performance of the proposed algorithm, the skull stripped ground truths of the CSF, GM and WM regions are shown in Fig. 4(b)–(d). Additionally,

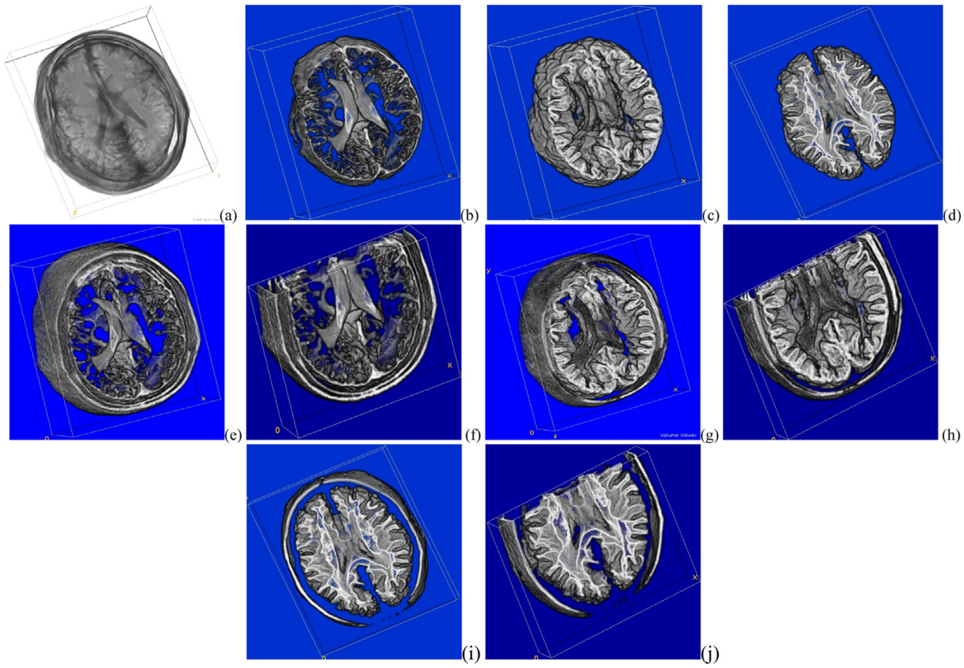

Fig. 4. Segmentation results on a T1-weighted (9% noise, 40% IIH) simulated 3D brain MR image volume. (a) 3D brain MR image volume, (b) Ground truth CSF image volume, (c) Ground truth GM image volume (d) Ground truth WM image volume, (e) Segmented CSF image volume, (f) Lower two-thirds portion of the CSF image volume, (g) Segmented GM image volume, (h) Lower two-thirds portion of the GM image volume, (i) Segmented WM image volume and (j) Lower two-thirds portion of the WM image volume.

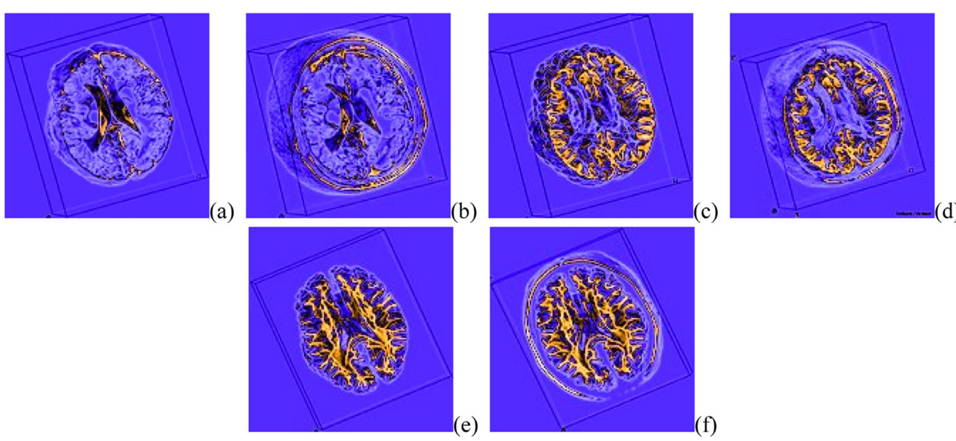

Fig. 5. 2D color mapped segmentation results on Fig. 4(a). (a) 2D color map of the ground truth CSF image volume, (b) 2D color map of the segmented CSF image volume (c) 2D color map of the ground truth GM image volume, (d) 2D color map of the segmented GM image volume, (e) 2D color map of the ground truth WM image volume and (f) 2D color map of the segmented WM image volume.

to make the results more informative, the 2D color mapped segmentation results along with the ground truths are shown in Fig. 5. While comparing the ground truths with the segmented image volumes of CSF, GM and WM regions, the results validate that the proposed algorithm efficiently segments the 3D brain MR image volume even with high levels of noise and IIH. In addition, these results also establish the fact that use of global entropy and spatially constrained likelihood-based local entropy in the FCMGsLE algorithm undermines the effect of noise and IIH while preserving the details of image volume. For better visualization of the segmented CSF, GM and WM regions the animated videos are presented in AnimatedCSF.gif, AnimatedGM.gif and AnimatedWM.gif, respectively.

3.2.2. Clinical brain MR image volumes

We have also collected four clinical brain MR image volumes from the EKO X-ray & Imaging Institute, Jawaharlal Nehru Road, Kolkata, India and the AMRI Hospital, Dhakuria, Kolkata, India to investigate the performance of the proposed algorithm. The resolution (height $\times$ width $\times$ depth) of these image volumes are 552 $\times$ 325 $\times$ 58 (Subject 1), 1105 $\times$ 649 $\times$ 20 (Subject 2), 256 $\times$ 150 $\times$ 20 (Subject 3) and 350 $\times$ 206 $\times$ 20 (Subject 4) and are acquired by 1.5T MRI machines. As these are real clinical brain MR image data, therefore they are believed to be more effected by noise and IIH.

Among the image volumes of four Subjects, Fig. 6 shows the segmentation results of Subject 1. Fig. 6(a) shows the image volume in 3D space; whereas, Fig. 6(b), (d) and (f) show the segmented image volumes of the CSF, GM and WM regions, respectively. Similar to the previous experiments, to get better view about the shapes and structures of these regions, we have shown the bottom two-thirds volumes of these regions in Fig. 6(c), (e) and (g), respectively. The Fig. 6(h)–(j) show the 2D color

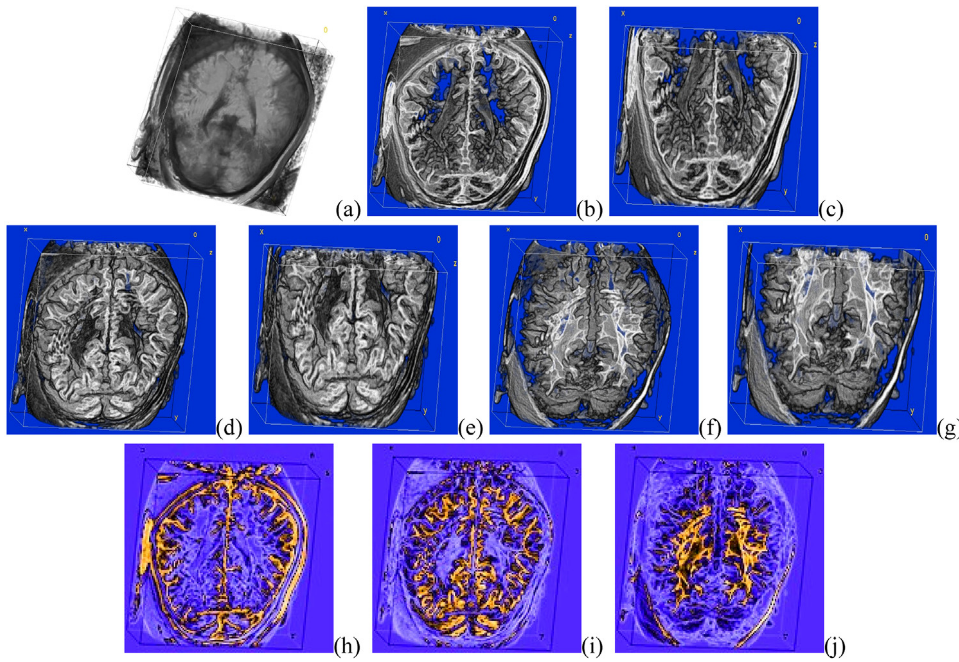

Fig. 6. Segmentation results on a clinical brain MR image volume. (a) Image volume, (b) Segmented CSF image volume, (c) Lower two-thirds portion of the segmented CSF image volume, (d) Segmented GM image volume, (e) Lower two-thirds of the segmented GM image volume, (f) Segmented WM image volume, (g) Lower two-thirds portion of the segmented WM image volume, (h) 2D color map of the segmented CSF image volume, (i) 2D color map of the segmented GM image volume and (j) 2D color map of the segmented WM image volume.

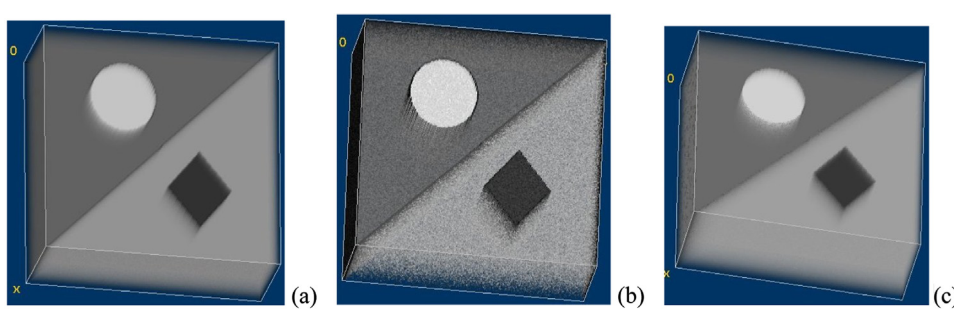

Fig. 7. Segmentation result on a synthetic image volume with Rician noise. (a) Synthetic image volume, (b) Image volume with Rician noise and (c) Segmented image volume of (b).

mapped segmentation results of the CSF, GM and WM regions, respectively.

The results again exhibit that the proposed FCMGsLE algorithm can effectively segment the different tissue regions of clinical 3D brain MR image volumes, thus validate its effectiveness.

3.2.3. Synthetic image volume

The voxel intensity in noisy 3D brain MR image volume is shown to be governed by a Rician distribution, resulting very low signal-to-noise ratio (SNR < 2) [26]. Therefore, the purpose of this experiment is to study the performance of the proposed FCMGsLE algorithm on a synthetic image volume with Rician noise. Accordingly, we have created a synthetic image volume of size $200 \times 200 \times 80$ (height $\times$ width $\times$ depth) having four dissimilar regions.

Fig. 7(a)–(b) show the synthetic image volume and its noisy image volume with Rician noise, respectively. Fig. 7(c) shows the segmented image volume by the FCMGsLE algorithm on Fig. 7(b). This result also further demonstrates that the FCMGsLE algorithm is capable of segmenting the synthetic image volume even with Rician noise.

3.3. Quantitative analysis

In addition to the above qualitative analysis, we have also performed quantitative analysis on the performance of the proposed FCMGsLE algorithm. Its performance is compared with that of the FCM [6] and its variants that incorporate (i) spatial information, namely sFCM [10], (ii) local spatial and gray-level information, namely FGFCM [8], (iii) adaptive spatial information, namely ASIFC [9], (iv) possibilistic information, namely PFCM [12] and global and local membership functions, namely 2sFMoF [14]. It may be noted that 2sFMoF algorithm works on 3D brain MR image volumes, while the others work on 2D image matrices.

3.3.1. Simulated 3D brain MR image volumes

Table 1 summarizes the segmentation accuracy of different algorithms while segmenting six volumes of simulated 3D brain MR image data. To investigate robustness of the algorithms in the presence of high levels of noise and IIH, the noise level is varied from 5%–9% and IIH from 20%–40%.

Results show that the 2sFMoF and proposed FCMGsLE algorithms yield better results than the other algorithms. Further, among the 18 cases, the 2sFMoF algorithm is found to be superior in 9 cases, while the FCMGsLE algorithm is in 8 cases. To

Table 1
Segmentation results of the proposed FCMGsLE algorithm and other competitive algorithms on simulated brain MR image volumes.

Volume (Noise%–IIH%)	Tissue regions	Segmentation accuracy (SA)						
		FCM	FGFCM	sFCM	ASIFC	PFCM	2sFMoF	FCMGsLE
5–20	CSF	0.881	0.861	0.907	0.911	0.907	**0.918**	0.867
	GM	0.834	0.828	0.916	0.919	0.879	**0.923**	**0.923**
	WM	0.848	0.941	0.938	0.946	0.959	0.968	**0.969**
5–40	CSF	0.837	0.832	0.861	0.867	0.875	**0.908**	0.873
	GM	0.825	0.821	0.909	0.911	0.837	**0.919**	0.911
	WM	0.840	0.916	0.926	0.933	0.925	**0.962**	0.932
7–20	CSF	0.819	0.816	0.852	0.859	0.836	**0.901**	0.876
	GM	0.818	0.801	0.902	0.907	0.815	0.911	**0.912**
	WM	0.829	0.909	0.912	0.918	0.949	0.954	**0.962**
7–40	CSF	0.807	0.795	0.849	0.852	0.817	**0.898**	0.883
	GM	0.782	0.792	0.895	0.889	0.772	0.902	**0.908**
	WM	0.795	0.906	0.903	0.908	0.926	**0.947**	0.924
9–20	CSF	0.753	0.739	0.827	0.836	0.777	**0.880**	0.878
	GM	0.755	0.736	0.871	0.875	0.762	0.894	**0.902**
	WM	0.781	0.873	0.897	0.901	0.932	0.942	**0.951**
9–40	CSF	0.742	0.731	0.824	0.829	0.753	0.876	**0.882**
	GM	0.742	0.725	0.862	0.868	0.737	0.879	**0.887**
	WM	0.765	0.876	0.873	0.880	0.914	**0.923**	0.910

Table 2
Statistical significance analysis of the FCMGsLE algorithm with other methods in terms of p-values for CSF, GM and WM regions for the results reported in Table 1.

Region		Paired t-test (one tailed)						
		FCMGsLE	2sFMoF	FCM	FGFCM	sFCM	ASIFC	PFCM
CSF	Mean of SA	0.877	0.897	0.807	0.796	0.853	0.859	0.828
	p-value	–	0.033	0.015	0.009	0.084	0.135	0.058
GM	Mean of SA	0.907	0.905	0.793	0.784	0.893	0.895	0.800
	p-value	–	0.184	0.000	0.000	0.012	0.019	0.000
WM	Mean of SA	0.941	0.949	0.810	0.904	0.908	0.914	0.934
	p-value	–	0.144	0.000	0.006	0.003	0.008	0.052

find whether the improvement in performance by the proposed FCMGsLE algorithm is significant, a statistical significance analysis is conducted by calculating paired t-test (one tailed) between the FCMGsLE and all other algorithms for all the tissue regions. In the process, we have set the null hypothesis H_0 as: 'the mean value of FCMGsLE is same as the compared method' against the alternative hypothesis H_1 as: 'the mean value of FCMGsLE is higher as compared to the related method'. We have presented summary of the findings in terms of mean values and p values in Table 2. From the analysis, it is found that for the CSF region, the proposed FCMGsLE algorithm is not superior to the 2sFMoF algorithm, as its mean value is lower than that of the latter one. However, its overall performance is better than the other algorithms and in particular, statistically significant over the FCM and FGFCM algorithms at $p = 0.05$. For GM region, the FCMGsLE algorithm is superior but not statistically significant over the 2sFMoF algorithm at $p = 0.05$. However, its performance is statistically significant over the all other algorithms at $p = 0.03$. Finally, for WM region, the FCMGsLE algorithm is not superior to the 2sFMoF algorithm. However, performance of the FCMGsLE algorithm is better and statistically significant over all other algorithms but PFCM method at $p = 0.03$.

Fig. 8 shows the Dice coefficient of the proposed FCMGsLE algorithm and other state-of-the-art algorithms over six volumes of T1-weighted simulated 3D brain MR images having noise (5%–9%) and IIH (20%–40%). The results show that the FCMGsLE algorithm performs equally well as compared to the 2sFMoF algorithm when level of noise is low. However, it outperforms all the algorithms when the presence of noise and IIH is high in the image volumes, thus demonstrates its superiority.

Figs. 9–10 show the partition coefficient and partition entropy of the FCMGsLE algorithm and other comparative algorithms on six T1-weighted simulated brain MR image volumes with 5%–9% noise and 20%–40% IIH. The results again establish that the proposed FCMGsLE algorithm is superior to all other state-of-the-art algorithms. In addition, its performance is closer to the ideal cases, as its partition coefficient and partition entropy are nearer to 1.0 and 0.0, respectively.

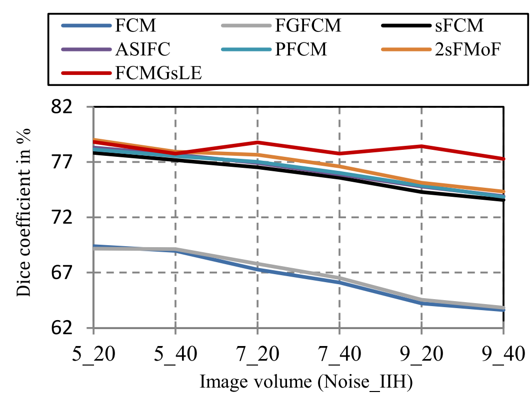

Fig. 8. Dice coefficient of different algorithms on six volumes of T1-weighted brain MR images by varying noise and IIH.

3.3.2. Clinical brain MR image volumes

This section presents the experimental study on four clinical 3D brain MR image volumes, as described Section 3.2.2. However, unlike the prior simulated brain MR image volumes, the ground truths are unavailable as these are the real clinical data. Therefore, among the four performance indices, the segmentation accuracy

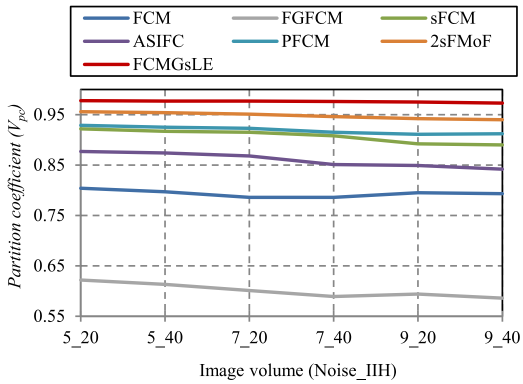

Fig. 9. Partition coefficient (V_{pc}) of different algorithms on six volumes of T1-weighted simulated brain MR images with 5%–9% noise and 20%–40% IIH.

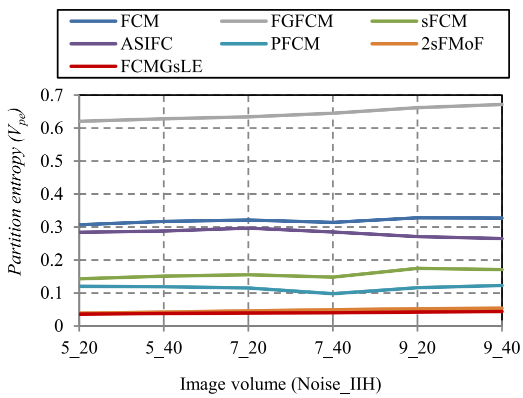

Fig. 10. Partition entropy (V_{pe}) of different algorithms on six volumes of T1-weighted simulated brain MR images with 5%–9% noise and 20%–40% IIH.

(SA) and Dice coefficient parameters are not applicable. Thus, we have presented the summary of the investigations in terms of partition coefficient and partition entropy of different algorithms in Table 3. The results again show that the proposed FCMGsLE algorithm is far superior to the other algorithms.

3.3.3. Synthetic image volume

We have also presented the segmentation results of the proposed FCMGsLE algorithm on the synthetic image volume with Rician noise, as described in Section 3.2.3, in Table 4. The results show that the FCMGsLE algorithm is capable of segmenting the different regions even with Rician noise. The results again demonstrate its efficiency and robustness to noise while segmenting the different regions.

In summary, by analyzing the different experimental studies we are certain that by using the global entropy and spatially constrained likelihood-based local entropy in the FCMGsLE algorithm, we can undermine the effect of noise and IIH while segmenting the noisy 3D brain MR image volumes.

3.4. Complexity analysis of the FCMGsLE algorithm

Let, the size of the noisy 3D brain MR image volume is $S = X \times Y \times Z(height \times width \times depth)$ and is required to segment it into C regions or clusters. Let, each voxel is represented by a d-dimensional feature vector. The FCMGsLE algorithm computes the global membership matrix $\boldsymbol{M}$ by calculating the norm distances between the cluster centers and the voxels of the 3D image volume. Therefore, the total time needed to calculate the membership matrix $\boldsymbol{M}$ is $O(dSC)$. In this study, we have considered only the voxel intensity value, giving $d = 1$ and $C = 4$ for CSF, GM, WM and background regions. Therefore, the total time required to calculate $\boldsymbol{M}$ is approximately $O(SC)$. Further, the local membership matrix $\boldsymbol{U}$ is calculated by computing the mean distance and the likelihood measure using the neighborhood B_T in $O(2B_T)$ for each voxel. Thus, for the image volume, this can be achieved in $O(2SB_T)$. Therefore, the total time required to calculate $\boldsymbol{U}$ is $O(SC + 2SB_T)$. Finally, the cluster centers are calculated in $O(SC)$. Therefore, for each iteration, the total time required to segment the 3D brain MR image volume is $O\,(SC + SC + 2SB_T + SC) = O(3SC + 2SB_T)$. The FCMGsLE algorithm takes 10–15 iterations to find the final cluster centers. The FCMGsLE algorithm is implemented in C programming language on a computer with Intel Core i7 @3.60 GHz CPU and 32 GB RAM running on Fedora 26 Linux environment. It takes approximately 300 s or 5 min to complete 15 iterations on a 3D brain MR image volume of size $181 \times 217 \times 51$.

In order to calculate the space complexity of the FCMGsLE algorithm, we need to consider its membership, distance and likelihood matrices, including those that hold temporary values and the input space. The space for the input image volume is $O(S)$.

Table 3
Partition coefficient (V_{pc}) and partition entropy (V_{pe}) of different algorithms on the clinical brain MR image volumes.

Volume	Method	V_{pc}	V_{pe}
Subject 1 (Female)	FCM	0.791	0.253
	FGFCM	0.811	0.159
	sFCM	0.835	0.074
	ASIFC	0.897	0.056
	PFCM	0.905	0.053
	2sFMoF	0.917	0.032
	FCMGsLE	0.987	0.023
Subject 2 (Female)	FCM	0.870	0.273
	FGFCM	0.893	0.193
	sFCM	0.907	0.178
	ASIFC	0.922	0.143
	PFCM	0.935	0.112
	2sFMoF	0.953	0.087
	FCMGsLE	0.987	0.022
Subject 3 (Female)	FCM	0.741	0.507
	FGFCM	0.852	0.287
	sFCM	0.883	0.228
	ASIFC	0.912	0.196
	PFCM	0.921	0.129
	2sFMoF	0.925	0.093
	FCMGsLE	0.986	0.024
Subject 4 (Male)	FCM	0.705	0.558
	FGFCM	0.815	0.329
	sFCM	0.886	0.294
	ASIFC	0.911	0.206
	PFCM	0.924	0.137
	2sFMoF	0.932	0.109
	FCMGsLE	0.987	0.022

Table 4
Segmentation results of the FCMGsLE algorithm on the synthetic image volume with Rician noise.

Index		Value
SA	Region 1	0.694
	Region 2	0.986
	Region 3	0.986
	Region 4	0.979
Dice coefficient		0.930
V_{pc}		0.988
V_{pe}		0.020

To compute global membership matrix $\boldsymbol{M}$, we need to use the distance matrix and also values of the global membership matrix, obtained in the previous iteration. Therefore, it requires a space $O\,(SC + SC + SC) = O(3SC)$. Similarly, the local membership matrix $\boldsymbol{U}$ also requires a space $O\,(SC + SC + SC) = O(3SC)$. The cluster center matrix requires a space $O(C)$. The final membership matrix $\boldsymbol{G}$ requires another space $O(SC)$. Therefore, the total memory space required for the FCMGsLE algorithm is $O(S + 3SC + 3SC + C + SC) \simeq O(7SC + S)$.

4. Conclusion

In summary, we have presented a novel entropy based fuzzy clustering algorithm to segment noisy 3D brain MR image volumes. In particular, the aim was to study the effectiveness of the fuzzy clustering algorithm that incorporates global entropy and spatially constrained likelihood-based local entropy while segmenting 3D brain MR image volumes with higher percentages of noise and IIH. The global entropy is defined using fuzzifier weighted global membership function; whereas, the local entropy is defined by the fuzzifier weighted local membership function, which is influenced by the reciprocal of spatially constrained likelihood-based possibility measure and the mean distance, calculated using the neighboring voxels and the cluster center. These entropies have better representation of the uncertainties that arise while classifying the voxels. The proposed algorithm judiciously incorporates these two membership functions as well as these two entropies into the fuzzy objective function. The solution of this objective function with the associated constraints is achieved by minimizing these entropies. The final membership function is obtained by thoughtfully combining these two membership functions. The experimental results based on six simulated and four clinical 3D brain MR image volumes, and a synthetic image volume with Rician noise suggest that the proposed FCMGsLE algorithm can effectively improve the segmentation results. In particular, in the presence of high noise and intensity inhomogeneity, it even yields far superior results than several state-of-the-art fuzzy clustering algorithms devised recently.

Declaration of competing interest

No author associated with this paper has disclosed any potential or pertinent conflicts which may be perceived to have impending conflict with this work. For full disclosure statements refer to https://doi.org/10.1016/j.asoc.2020.106171.

CRediT authorship contribution statement

Nabanita Mahata: Conceptualization, Investigation, Methodology, Validation, Visualization, Writing - original draft. **Jamuna Kanta Sing:** Conceptualization, Methodology, Funding acquisition, Project administration, Supervision, Validation, Writing - review & editing.

Acknowledgments

This work is partially supported by the SERB, Govt. of India (File No: EEQ/2016/000145). We are also thankful to the radiologists Dr. S.K. Sharma and Dr. Sumita Kundu of EKO X-ray & Imaging Institute, Jawaharlal Nehru Road, Kolkata, India for giving us the clinical brain MR images. We are also tankful to Mr. Banshadhar Nandi and Mr. Niloy Haldar, Sr. Technologist (Imaging), AMRI Hospital, Dhakuria, Kolkata, India for generous help and giving clinical brain MR images.

References

[1] U. Vovk, F. Pernujs, B. Likar, A review of methods for correction of intensity inhomogeneity in MRI, IEEE Trans. Med. Imaging 26 (2007) 405–421.
[2] Z. Hou, A review on MR image intensity inhomogeneity correction, Int. J. Biomed. Imaging 2006 (2006) 1–11.
[3] M.A. Balafar, A.R. Ramli, M.I. Saripan, S. Mashohor, Review of brain MRI image segmentation methods, J. Artif. Intell. 33 (2010) 261–274.
[4] B. Belaroussi, J. Millesb, S. Carmec, Y.M. Zhua, H. Benoit-Cattin, Intensity non-uniformity correction in MRI: Existing methods and their validation, Med. Image Anal. 10 (2006) 234–246.
[5] L. Dora, S. Agrawal, R. Panda, A. Abraham, State-of-the-art methods for brain tissue segmentation: A review, IEEE Rev. Biomed. Eng. 10 (2017) 235–249.
[6] J.C. Bezdek, Pattern Recognition with Fuzzy Objective Function Algorithms, Kluwer academic publishers, Norwell, MA, USA, 1981.
[7] M.N. Ahmed, S.M. Yamany, N. Mohamed, A.A. Farag, T. Moriarty, A modified fuzzy c-means algorithm for bias field estimation and segmentation of MRI data, IEEE Trans. Med. Imaging 21 (2002) 193–199.
[8] W. Cai, S. Chen, D. Zhang, Fast and robust fuzzy c-means clustering algorithms incorporating local information for image segmentation, Pattern Recognit. 40 (2007) 835–838.
[9] Z. Wang, Q. Song, Y.C. Soh, K. Sim, An adaptive spatial information-theoretic fuzzy clustering algorithm for image segmentation, Comput. Vis. Image Underst. 117 (2013) 1412–1420.
[10] K.S. Chuang, H.L. Tzeng, S. Chen, J. Wu, T.J. Chen, Fuzzy c-means clustering with spatial information for image segmentation, Comput. Med. Imaging Graph. 30 (2006) 9–15.
[11] C. Qiu, J. Xiao, L. Yu, L. Han, M.N. Iqbal, A modified interval type-2 fuzzy c-means algorithm with application in MR image segmentation, Pattern Recognit. Lett. 34 (2013) 1329–1338.
[12] N.R. Pal, K. Pal, J.M. Keller, J.C. Bezdek, A possibilistic fuzzy c-means clustering algorithm, IEEE Trans. Fuzzy Syst. 13 (2005) 517–530.
[13] N. Mahata, S. Kahali, S.K. Adhikari, J.K. Sing, Local contextual information and Gaussian function induced fuzzy clustering algorithm for brain MR image segmentation and intensity inhomogeneity estimation, Appl. Soft Comput. 68 (2018) 586–596.
[14] S. Kahali, S.K. Adhikari, J.K. Sing, A two-stage fuzzy multi-objective framework for segmentation of 3D MRI brain image data, Appl. Soft Comput. 60 (2017) 312–327.
[15] J.K. Sing, S.K. Adhikari, D.K. Basu, A modified fuzzy c-means algorithm using scale control spatial information for MRI image segmentation in the presence of noise, J. Chemom. 29 (2015) 492–505.
[16] S.K. Adhikari, J.K. Sing, D.K. Basu, M. Nasipuri, Conditional spatial fuzzyc-means clustering algorithm for segmentation of MRI images, Appl. Soft Comput. 34 (2015) 758–769.
[17] S. Pereira, A. Pinto, V. Alves, C.A. Silva, Brain tumour segmentation using convolutional neural networks in MRI images, IEEE Trans. Med. Imaging 35 (2016) 1240–1251.
[18] P. Moeskops, M.A. Viergever, A.M. Mendrik, L.S. Vries, M.J.N.L. Benders, I. Isgum, Automatic segmentation of MR brain images with a convolutional neural network, IEEE Trans. Med. Imaging 35 (2016) 1252–1262.
[19] J. Yao, M. Dash, S.T. Tan, H. Liu, Entropy-based fuzz clustering and fuzzy modeling, Fuzzy Sets and Systems 113 (2016) 1240–1251.
[20] M. Zarinbal, M.H. Fazel Zarandi, I.B. Turksen, Relative entropy fuzzy c-means clustering, Inform. Sci. 260 (2014) 74–97.
[21] S. Askari, N. Montazerin, M.H. Fazel Zarandi, E. Hakimi, Generalized entropy based possibilistic fuzzy c-means for clustering noisy data and its convergence proof, Neurocomputing 219 (2017) 186–202.
[22] S.R. Kannan, S. Ramathilagam, P.C. Chung, Effective fuzzy c-means clustering algorithms for data clustering problems, Expert Syst. Appl. 39 (2012) 6292–6300.
[23] R.R. Gharieb, G. Gendy, A. Abdelfattah, C-means clustering fuzzified by two membership relative entropy functions approach incorporating local data information for noisy image segmentation, SIViP 11 (2017) 541–548.
[24] K.-L. Wu, Analysis of parameter selections for fuzzy c-means, Pattern Recognit. 45 (2012) 407–415.
[25] C.A. Cocosco, V. Kollokian, K.R.K.S. Kwan, A.C. Evans, Brainweb: Online interface to a 3D MRI simulated brain database, Neuroimage 5 (1997) 425.
[26] H. Gudbjartsson, S. Patz, The Rician distribution of noisy MRI data, Magn. Reson. Med. 34 (1995) 910–914.